OAK RIDGE NATIONAL LABORATORY LIBRARIES
3 4456 0599457 7

ORNL/TM-6995

ornl

OAK
RIDGE
NATIONAL
LABORATORY

UNION
CARBIDE

Tensile and Creep Behavior of Type 308 CRE Stainless Steel Joining 13-mm Type 304 Stainless Steel Plate

R. W. SWINDEMAN
E. BOLLING
R. T. KING

OAK RIDGE NATIONAL LABORATORY
CENTRAL RESEARCH LIBRARY
CIRCULATION SECTION
4500N ROOM 175
LIBRARY LOAN COPY
DO NOT TRANSFER TO ANOTHER PERSON
If you wish someone else to see this report, send in name with report and the library will arrange a loan.
UCN-7969 3 9-77

[redacted]

OPERATED BY
UNION CARBIDE CORPORATION
FOR THE UNITED STATES
DEPARTMENT OF ENERGY

Printed in the United States of America. Available from
the Department of Energy
Technical Information Center
P.O. Box 62, Oak Ridge, Tennessee 37830
Printed Copy A03 ; Microfiche A01

This report was prepared as an account of work sponsored by an agency of the United States Government. Neither the United States nor any agency thereof, nor any of their employees, makes any warranty, expressed or implied, or assumes any legal liability or responsibility for any third party's use or the results of such use of any information, apparatus, product or process disclosed in this report, or represents that its use by such third party would not infringe privately owned rights.

ORNL/TM-6995
Distribution
Category UC-79b, -h, -k

Contract No. W-7504-eng-26

METALS AND CERAMICS DIVISION

TENSILE AND CREEP BEHAVIOR OF TYPE 308 CRE STAINLESS STEEL JOINING 13-mm TYPE 304 STAINLESS STEEL PLATE

R. W. Swindeman, E. Bolling, and R. T. King

Date Published: November 1979

NOTICE This document contains information of a preliminary nature. It is subject to revision or correction and therefore does not represent a final report.

OAK RIDGE NATIONAL LABORATORY
Oak Ridge, Tennessee 37830
operated by
UNION CARBIDE CORPORATION
for the
DEPARTMENT OF ENERGY

CONTENTS

ABSTRACT. 1
INTRODUCTION. 1
MATERIAL PREPARATION. 2
Test Methods 9
RESULTS 9
Tensile Tests. 9
Creep-Rupture. 11
Representation of the Creep Curve. 16
DISCUSSION. 20
CONCLUSIONS 23
ACKNOWLEDGMENTS 23
REFERENCES. 23

TENSILE AND CREEP BEHAVIOR OF TYPE 308 CRE STAINLESS STEEL JOINING 13-mm TYPE 304 STAINLESS STEEL PLATE*

R. W. Swindeman, E. Bolling, and R. T. King†

ABSTRACT

As part of an effort to develop and validate design technology for use in the Liquid-Metal Fast Breeder Reactor (LMFBR) Program, we are studying creep and crack growth in weldments. In one set of experiments the weldments were fabricated by joining 13-mm (1/2-in.) plates of a reference heat of type 304 stainless steel by manual shielded metal-arc welding (SMAW) using type 308 controlled residual elements (CRE) filler metal. To analyze the behavior of the weldments we gathered uniaxial test data from specimens cut from the weldments. Tensile and creep tests were performed on these specimens at 593°C (1100°F).

On examination properties in the longitudinal (all weld metal) orientation differed significantly from those in the transverse (composite) orientation; the longitudinal orientation had superior creep-rupture properties. This was partly because the transverse (composite) weldment contained some weaker base metal. We developed a creep law to represent the strain-time behavior of the longitudinal weld metal specimens for times to 36 Ms (10,000 h).

INTRODUCTION

The need to develop an improved high-temperature design methodology for use in the U.S. Liquid-Metal Fast Breeder Reactor (LMFBR) Program was recognized in the late sixties. To satisfy this need the U.S. Department of Energy (USAEC at that time) initiated a national effort to study problems specific to the LMFBR. Very early, weldments were identified as a critical area for research and development. Several national laboratories and government contractors undertook cooperative programs to accomplish the following goals: (1) compile and evaluate the existing data on austenitic stainless steel welds,[1] (2) optimize the welding processes and weld deposited chemical compositions to produce sound weldments with properties comparable or superior to base metal,[2] (3) establish inelastic analysis methods

*Work performed under DOE/RRT AG 10 20 42 4, Task 02, (OH048), "High-Temperature Structure Design."

†Present address: Sprague Electric Company, Marshall Street, North Adams, MA 01247.

and design criteria,[3] (4) develop a data base for use in long-time high-temperature design,[4] and (5) validate the high-temperature design methodology by performing structural tests.[5]

A high priority was assigned to weldments produced with type 308 stainless steel filler metal because of its use in fabricating the vessel and piping for the Fast-Flux Test Facility (FFTF). Combustion Engineering produced the vessel and joined Oak Ridge National Laboratory (ORNL) in a program to develop an improved version of type 308. The result of the effort was a subclass of filler metal, type 308 CRE stainless steel, which contained three controlled residual elements: boron (about 0.007%), titanium (about 0.06%), and phosphorus (about 0.04%). The development of this material is described by Binkley, King, and co-workers.[2,4,6–8]

There has been a substantial effort to produce a data base for type 308 CRE stainless steel. King and co-workers[4,7–9] have determined elastic, tensile, and creep-rupture properties, while Brinkman and Korth[10] and others[11,12] have studied fatigue and creep-rupture behavior. Furthermore, Westinghouse Advanced Reactor Division (WARD) has attempted to study the performance of type 308 CRE stainless steel in "basic specimen" and "structures"[5,13] tests. It should be recognized that the mechanical behavior of a weld material is controlled by more that just the chemical composition. The joint design and welding techniques also play an extremely important role. For this reason the type 308 CRE weldment data produced in the materials programs were judged to be unrepresentative of weld material as deposited in the weldments supplied to WARD by ORNL. A separate set of "characterization data" was needed. This report summarizes the uniaxial tests performed on coupons machined from the weldments produced for WARD.

MATERIAL PREPARATION

Welds were made by joining 13-mm-thick (1/2-in.) plates of type 304 stainless steel (heat 9T2796). The sawing plan for the plates is shown in Fig. 1. Twenty-eight plates measured 254 by 76.2 mm (10 by 3 in.) with the long dimension parallel to the primary rolling direction. Eighteen plates measured 152 by 127 mm (6 by 5 in.) with the long direction transverse to the primary rolling direction. Six small plates measured 152 by 60.3 mm (6 by 2 3/8 in.) with the long direction transverse to the primary rolling direction.

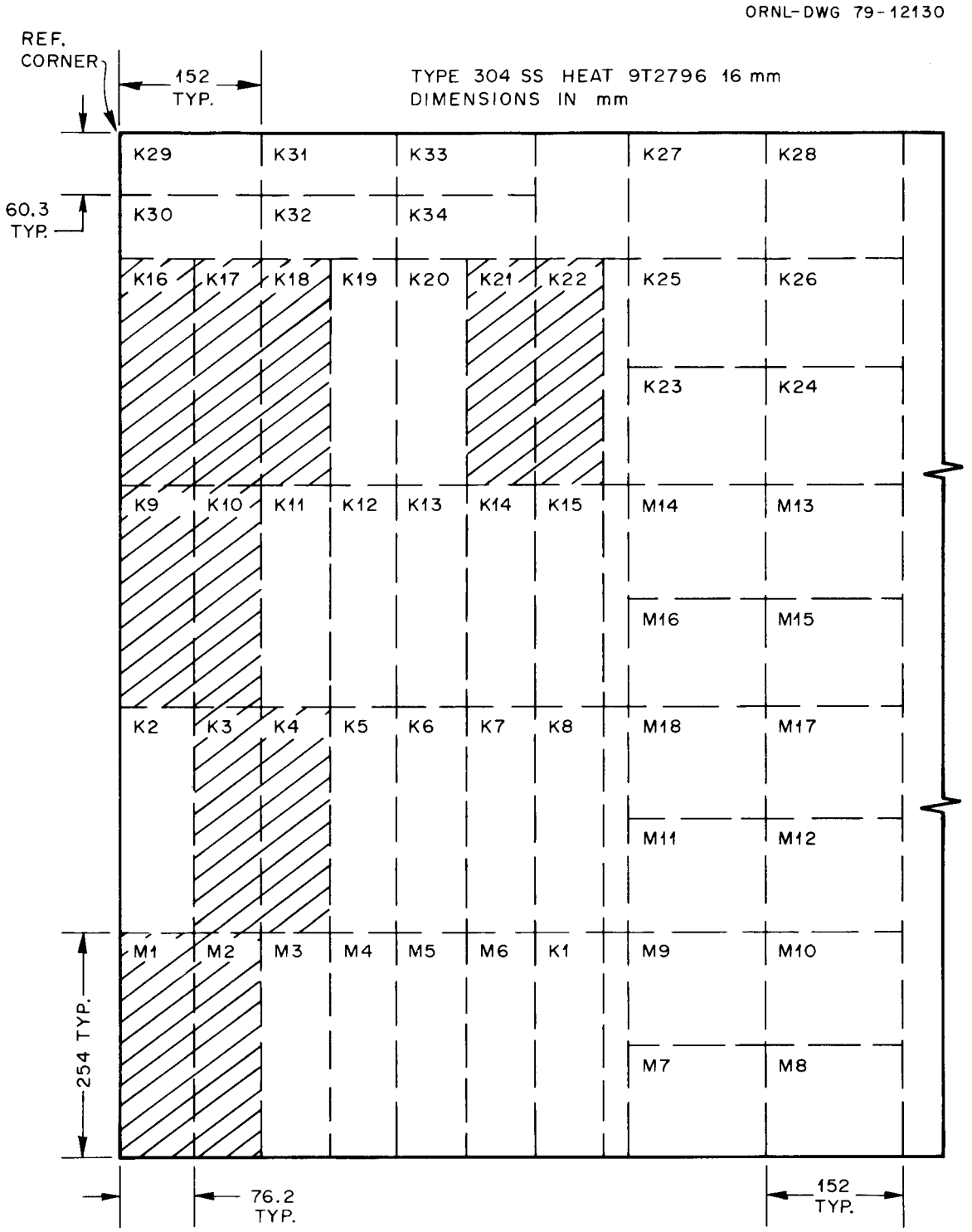

Fig. 1 Sawing Plan for Plates Used to Fabricate Weldments. Shaded area represents plates used for uniaxial characterization tests.

Two matching plates were strapped to the fixture sketched in Fig. 2. The fixture contained a backup plate clad with a 9.53-mm (3/8-in.) overlay of the same type 308 CRE stainless steel used to weld the plates. The weld-joint design bore little resemblance to joint designs typical for 13-mm (1/2-in.) plates. Rather, it was designed to deposit at least a 13-mm (1/2-in.) width of weld metal between two beveled surfaces. The design is sketched in Fig. 3.

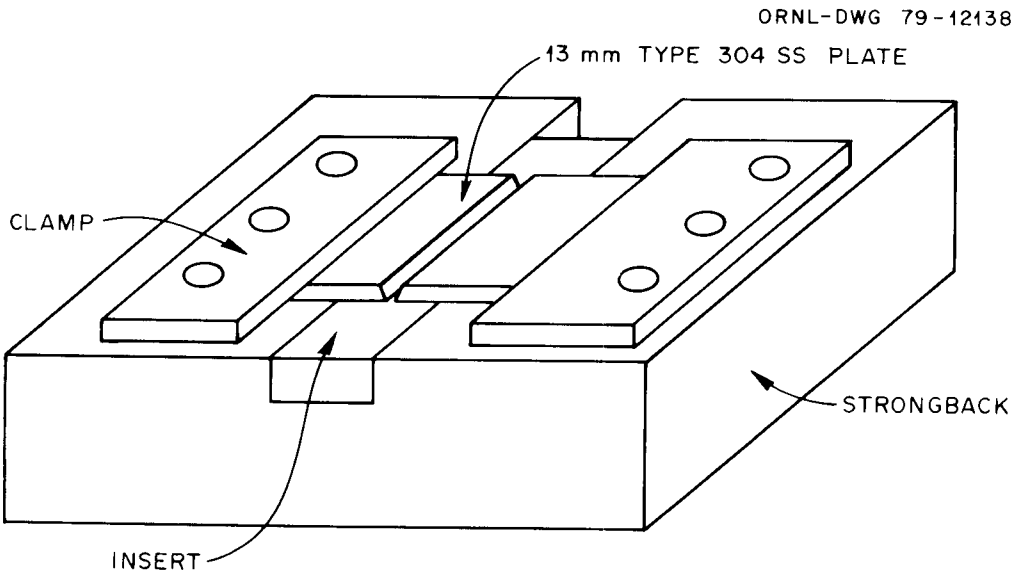

Fig. 2. Diagram of Welding Fixture.

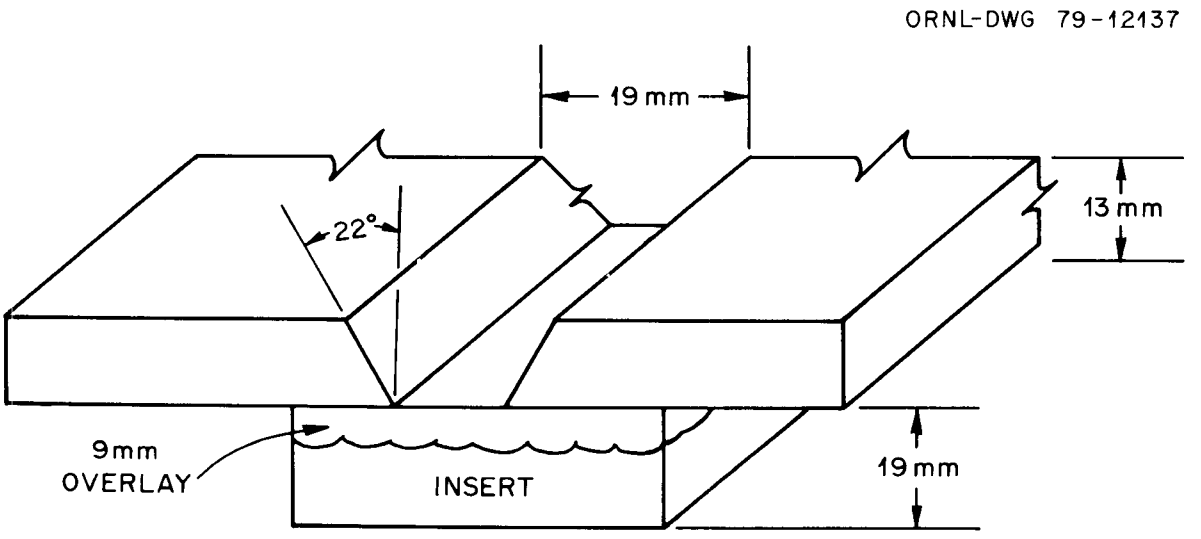

Fig. 3. Setup for Welding.

The weld metal was deposited by the shielded metal-arc process with 6.35-mm-diam (0.25-in.) electrodes. Four or five passes were required. The electrodes were from batch ABHB of type 308 CRE stainless steel. The chemical compositions of the ABHB electrode, a typical FFTF electrode, and the wrought 13-mm (1/2-in.) plate are listed in Table 1.

Table 1. Analysis of Types 304 and 308 CRE Stainless Steel Used to Fabricate Weldments

Element	Content, wt %		
	Type 304[a]	Type 308 CRE	
	Heat 9T2796	Lot ABHB	Lot HBEA
Si	0.48	0.46	0.56
S	0.015	0.007	0.005
P	0.028	0.043	0.040
Mn	1.22	1.77	1.83
C	0.052	0.060	0.064
Cr	18.6	19.50	19.70
Ni	9.7	9.48	9.61
Mo	0.32	0.20	0.07
Nb + Ta	0.003	<0.01	<0.01
Ti	0.01	0.06	0.06
Co	0.18	0.06	0.03
Cu	0.24	0.11	0.04
B		0.007	0.007
V		0.09	0.07
N	0.052	0.041	0.03

[a]Ladle analysis except for carbon and nitrogen.

A macroscopic cross section of a typical weld is shown in Fig. 4(a). The weld region near the backup plate (root) was about 13 mm (1/2 in.) wide, while the region near the top (face) was typically 22 mm (9/10 in.) wide. Thus, the weld had a taper in the thickness direction of the plate. Microhardness data are also shown in Fig. 4. The hardness increased systematically from the face (DPH 220) to the root (DPH 275) [see Fig. 4(b)]. A substantial variation in hardness was also detected in the width direction. For example, the base metal away from the fusion line exhibited around DPH 210, while hardness near the weld centerline varied widely but was in the range 230 to 260 DPH [see Fig. 4(c)]. Comparison of hardness in this weld to data for the FFTF weld metal used

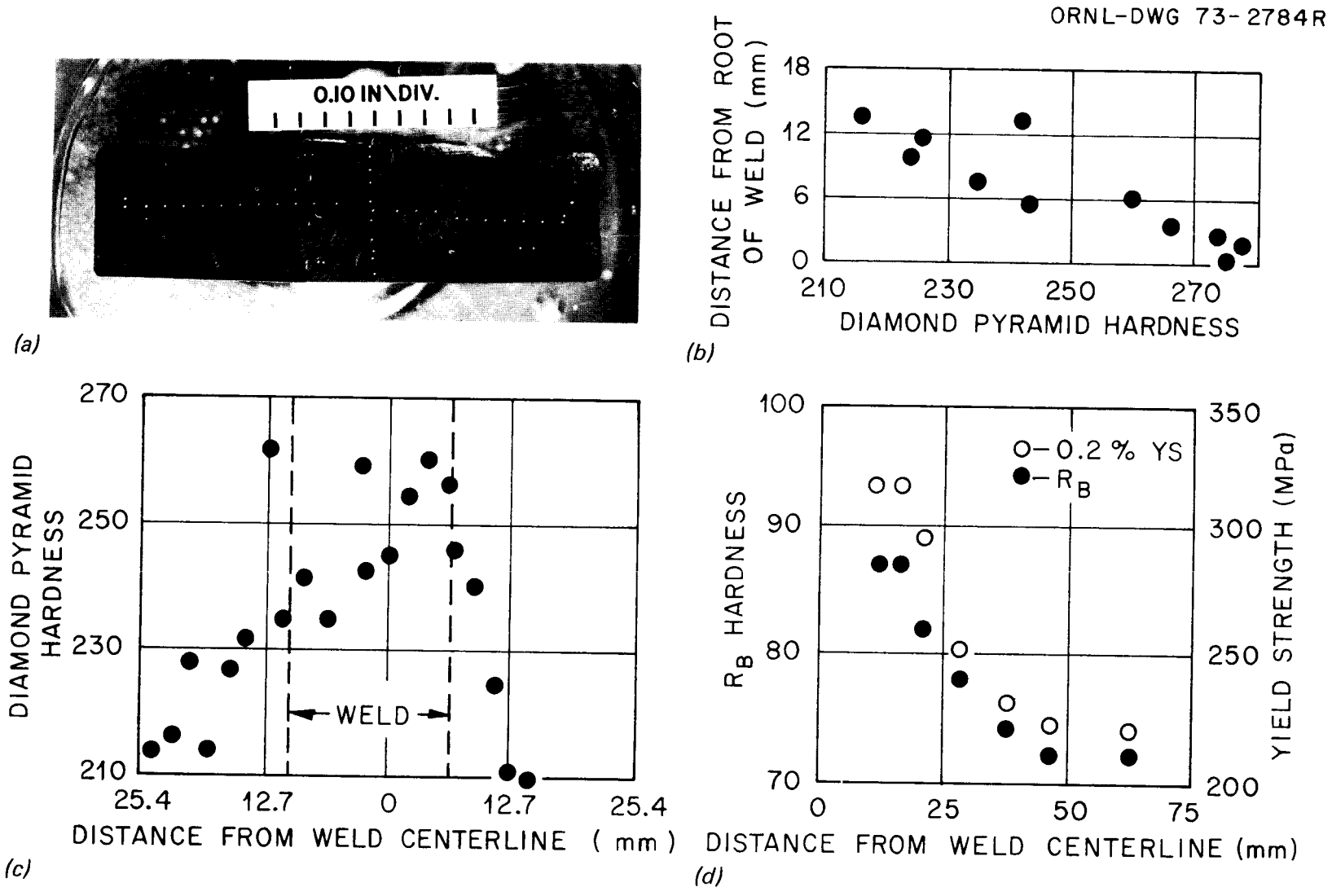

Fig. 4. Hardness Traverses of Type 308 CRE Weldment in 13-mm (1/2-in.) 304 Stainless Steel Plate.

in the data generation program[4] indicated that both types of welds had varied similarly from maximum hardness to minimum hardness. We also determined a Rockwell B hardness profile for the 13-mm (1/2-in.) plate with equivalent yield strengths. Data are shown in Fig. 4(d).

The allocation of the plates after welding is indicated in Fig. 1. The shaded regions represent plates retained at ORNL for characterization testing. The other plates were shipped to M. J. Manjoine[5] for use in the WARD program. The sawing plan for producing specimen blanks in the ORNL plates is indicated in Figs. 5 through 7. Plates M1/M2, K3/K4, K9/K10, K17/K18, and K21/K22 were sectioned according to the scheme in Fig. 5.

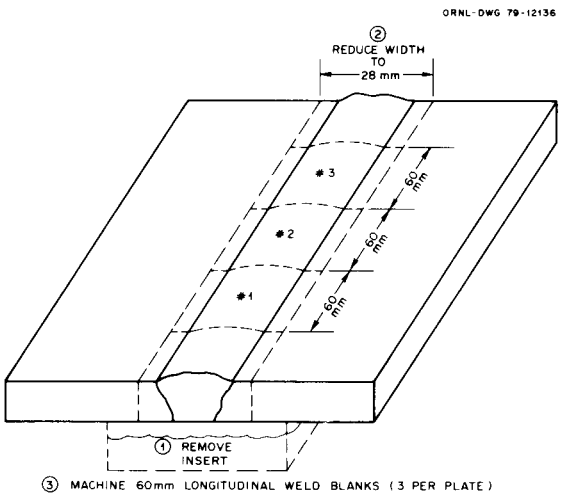

Fig. 5. Sawing Plan for Plates M1/M2, K3/K4, K9/K10, K17/K18, and K21/K22.

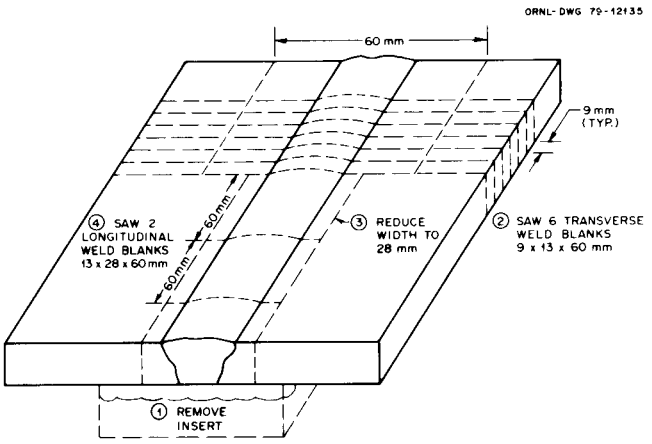

Fig. 6. Sawing Plan for Plate K15/K16.

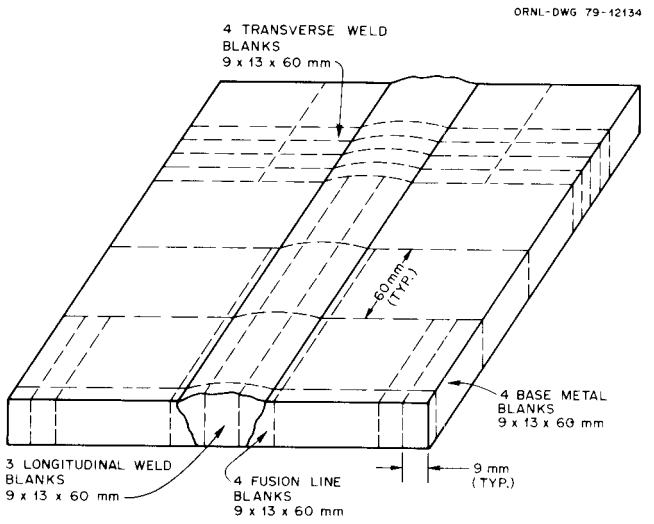

Fig. 7. Sawing Plan for Plate K11/K12.

This consisted of: (1) machining away the insert blank, (2) reducing the as-welded plate width to contain only the center 28 mm (1.1 in.), and (3) transverse sectioning of the plate to produce three 60-mm-long (2 3/8-in.) and two short end pieces. The 5 plates provided 15 specimen blanks parallel to the welding direction (longitudinal orientation). Plate K15/K16 was sectioned according to Fig. 6. Here two longitudinal blanks were produced by sectioning the same way as before (Fig. 5). However, the remainder was cut into six blanks transverse to the weld. Each blank was 9- by 13- by 60-mm (3/8- by 1/2- by 2 3/8-in.) long. The weld was in the center of the 60-mm length. Plate K11/K12 was sectioned as follows: 9- by 13- by 60-mm-long (3/8- by 1/2- by 2 3/8-in.) blanks, were sawed from the base metal near the plate corners, three 9- by 13- by 60-mm (3/8- by 1/2- by 2 3/8-in.) all-weld-metal blanks were sawed in the longitudinal direction, four "fusion-line" blanks of identical dimensions were sawed from regions adjacent to the longitudinal weld metal blanks, and four blanks transverse to the weld were sawed with the same dimensions as the transverse blanks obtained from plate K15/K16 (Fig. 6). In total, 20 longitudinal and 10 transverse weld metal, 4 base metal, and 4 fusion-line specimen blanks were produced.

All but seven of the specimen blanks were used to fabricate threaded-end bar specimens 6.35 mm (0.25 in.) in diameter by 32 mm (1.25 in.) in reduced section length. Smaller button head specimens were machined from

the remaining seven specimen blanks of longitudinal weld metal. These specimens had 6.35-mm-diam (0.25-in.) shoulders 3.17 mm (0.125 in.) in gage diameter and 29 mm (1.125 in.) in reduced section length. Three specimens were machined from the center of the weld (halfway through the thickness). Two were machined from material at the top 1/4 thickness and the remaining two from material near the weld root (3/4 thickness).

Test Methods

All testing was performed at 593°C (1100°F). Tensile tests were conducted in a 44-kN (10,000-lb) Instron machine at a nominal crosshead speed of 0.002 mm/s (8.3×10^{-5} in./s). The nominal strain rate was close to 6.7×10^{-5}/s. Creep-rupture tests were performed in 12:1 lever arm machines. Extensometers were attached to the specimen shoulders.

RESULTS

Tensile Tests

The results of tensile tests are provided in Table 2. With regard to the variation through the thickness, the specimen from the face (1/4 thickness) had the lowest yield strength, while the specimen from the root (3/4 thickness) had the highest yield strength. The ultimate strengths and uniform strains were about the same for all three locations, while the fracture strain was highest for the face specimen and lowest for the root specimen. These data became less credible when we examined data for 6.3-mm-diam (0.25-in.) specimens. Supposedly, data from these specimens represented center behavior, yet the yield strengths for duplicate samples fell below the yield strengths for the face specimen. The larger diameter specimens produced about the same ultimate strength and slightly more uniform strain than smaller diameter specimens. The transverse weld specimen exhibited slightly higher yield and ultimate strengths and much less uniform elongation, total strain, and reduction of area than the 6.3-mm-diam (0.25-in.) longitudinal weld specimen. The six tests exhibited an average yield strength near 180 MPa (26.2 ksi). This strength was much in excess

Table 2. Summary of Tensile Tests on WARD Weld Specimens

Specimen	Specimen Type	Strength, MPa(ksi)			Uniform Strain (%)	Elongation (%)	Reduction of area (%)
		0.2% Yield	Ultimate	True Ultimate			
LWM 1-1	Long. Face	178(25.8)	283(41.1)		23.4	28.8	60.0
LWM 2-1	Long. Center	186(27.2)	282(40.9)		25.2	34.1	60.0
LWM 3-1	Long. Root	199(28.8)	290(42.1)		24.0	34.3	53.5
LWM 6	Long. Center	273(25.1)	292(42.3)	378(54.8)	29.4	39.6	62.8
LWM 7	Long. Center	163(23.7)	295(42.8)	378(54.8)	28.1	39.5	71.6
LWM 2	Trans. Center	183(26.5)	312(45.3)	360(52.3)	15.5	21.5	47.2

of the 120-MPa (17.4-ksi) average yield strength for mill-annealed type 304 stainless steel.[14] No tensile data for the 13-mm (1/2-in.) mill-annealed plate were obtained at 593°C (1100°F). However, the yield strength at room temperature was determined to be in the range 202 to 227 MPa (29.3 to 32.9 ksi).[15] Typically, a material with this range of room temperature yield strength would yield at around 100 MPa (14.5 ksi) at 593°C (1100°F).[14] Thus, if the room temperature yield is accurate, the weld metal was about 80% stronger than the base metal away from the weld. However, the base metal DPH values (Fig. 4) were around 210 and the R_B values were high [Fig. 4(d)]. These hardness data imply a room temperature yield stress for the base metal around 310 MPa (45 ksi). The corresponding yield strength at 593°C (1100°F) would be 175 MPa (25 ksi), which is closer to the weld metal strength. Full stress-strain curves for the weld metal for longitudinal and transverse FFTF weld specimens and for reannealed base metal are plotted in Fig. 8. As mentioned earlier, the yield strengths of the transverse and longitudinal welds were about the same. This is true for both FFTF and WARD welds. The transverse weld metal hardens more rapidly during the first few percent strain. As a consequence, the transverse weld specimens are much stronger than longitudinal weld specimens in the 2 to 15% strain range. The FFTF welds specimens were taken from "level 1" or near surface location but still exhibited greater strengths than the specimens machined from WARD weldments. Figure 8 clearly shows the vast difference at low strains in flow stress of the weld material and the reannealed 13-mm (1/2-in.) plate. Eventually, the reannealed plate hardens to stresses comparable to the weld specimens, but not until 15 or 20% strain is introduced.

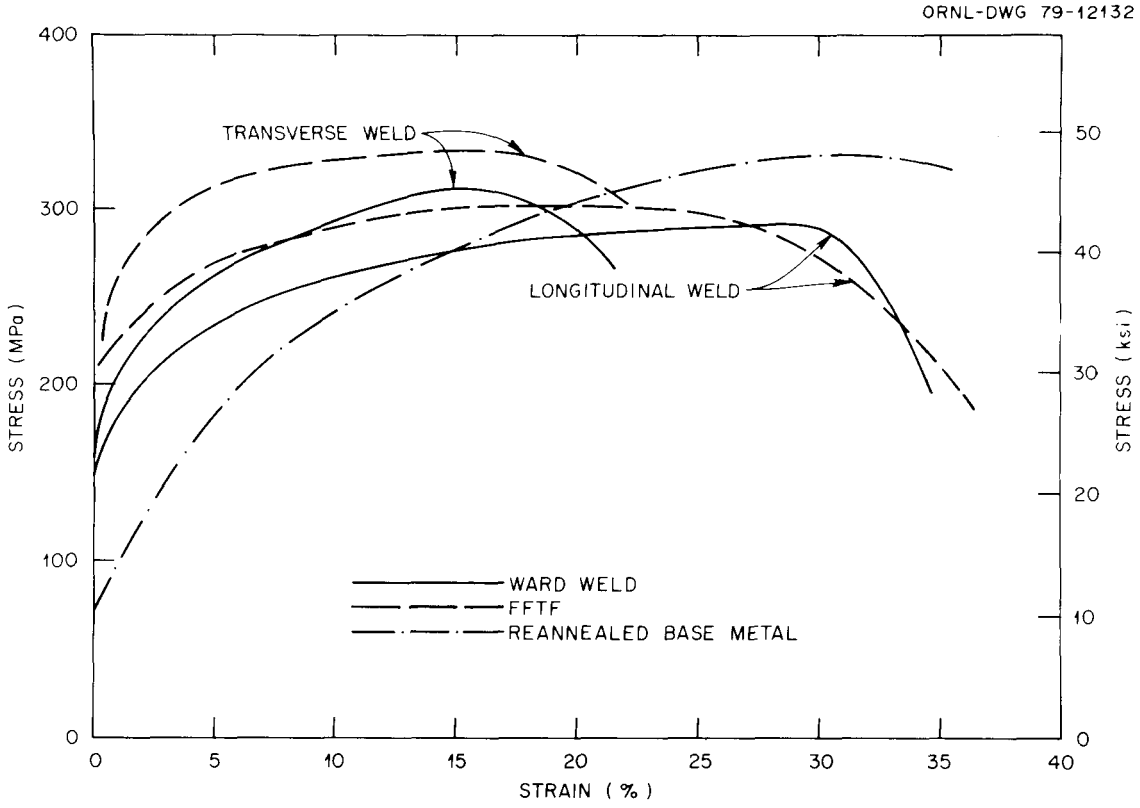

Fig. 8. Comparison of Stress vs Strain Curves for Type 308 CRE Stainless Steel Welds in 13-mm (1/2-in.) Plate with Curves for FFTF Welds and Type 304 Stainless Base Metal at 593°C (1100°F).

Creep-Rupture

Creep-rupture tests are summarized in Table 3. Included are seven tests on longitudinal weld metal, five tests on transverse weldments, two tests on fusion-line material, and three tests on base metal. Stresses are in the range 124 to 241 MPa (18 to 35 ksi), and times fall in the range 21 ks to 64 Ms (6 to 18,000 h). Tests in excess of 172 MPa (25 ksi) should be considered "characterization tests" since the stresses are too high to be of much value in the analysis of structures, except if we are concerned with sharp notches or cracks where the theoretical elastic stress could exceed 172 MPa (25 ksi).

The loading strains from the creep tests are compared to the tensile curves for transverse and longitudinal orientations in Fig. 9. Data exhibit scatter but fall in the range between the two tensile curves with only two exceptions.

Table 3. Summary of Creep Tests Performed on Manjoine (WARD) Specimens

Test	Stress (MPa)	Stress (ksi)	Time[a] (h)	Strain, % Loading e_L	Strain, % Transient e_t	Strain, % Rupture e_R	Minimum Strain Rate $\dot{e}_m$ (%/h)	Reduction of Area (%)
				Longitudinal Weld Metal				
185	241	35	48.8R	5.5	5.0	48	0.54	57
186	220	32	237.6R	2.9	6.0	47	0.10	55
184	207	30	1850.4R	0.96	2.4	46	0.03	54
187	193	28	3488.3R	1.62	3.13	35	0.002	52
183	172	25	12700R	0.54	~0.7	35	0.00045	
271	138	20	18118D	0.23	0.23	>0.6	0.00001	
272	124	18	4058D	0.06	>0.11	>0.3	>0.00003	
				Transverse Weld Metal				
276	220	32	86.4R	0.73	1.4	21	0.03	
188	220	32	85.7R	2.45	1.4	13	0.082	11
190	193	28	317.2R	0.40	0.30	10	0.016	6
189	172	25	752.9R	0.13	0.25	7.1	0.001	9
279	138	20	5731D	0.25	1.5	>2	0.0002	
				Fusion-Line Metal				
274	207	30	312.5R	0.42	0.04	31		
278	138	20	15265D	0.16	0.34	>2.7	0.000042	
				Base Metal				
273	241	35	6D	6.5	0.5	31		
280	207	30	257.9R		1.5	25	0.065	
275	124	18	13483D	0.53	3.0	>4.5	0.00007	

[a]R—time specimen ruptured; D—time test discontinued.

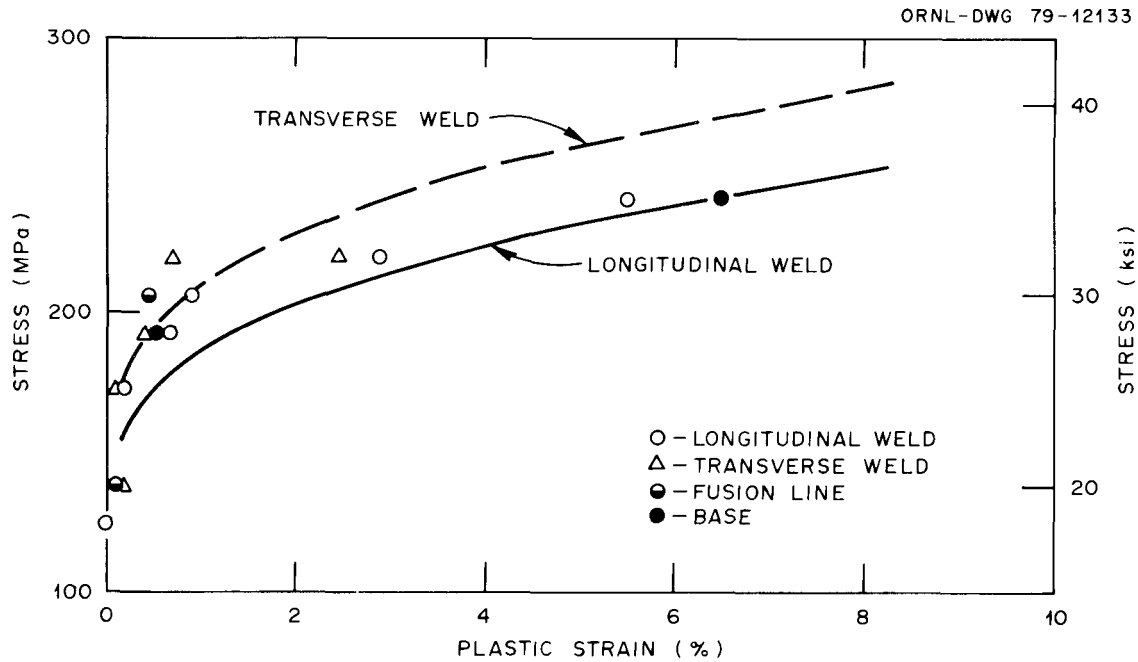

Fig. 9. Comparison of Creep Loading Strains for Weld Metal Specimens with Tensile Curves at 593°C (1100°F).

Stress-rupture data are plotted in Fig. 10. Specimens machined in the longitudinal weldment orientation lasted longer than those machined in the transverse direction. There was also a big difference in rupture ductilities (given as numbers in Fig. 10). The longitudinal weld specimens were very ductile (at least 30% elongation), while the transverse weld specimens exhibited lower ductility (no more than 13% elongation). The fusion-line and base metal specimens exhibited properties between the two extremes described above. The transverse weldment appeared to fail in the base metal. The stress versus rupture life behavior for longitudinal weldments was comparable to the behavior of level 1 longitudinal welds in the FFTF vessel. These data, as well as data for the laboratory reannealed 13-mm (1/2-in.) plate, are included in Fig. 10. We see that the reannealed material was weak relative to the weldment and mill-annealed 13-mm (1/2-in.) plate.

Secondary creep rate data from Table 3 are plotted in Fig. 11. Again, the longitudinal weld specimens were stronger than the transverse weld specimens. The fusion-line specimen was also strong, while the base metal and transverse weld materials were weaker and relatively equivalent. When

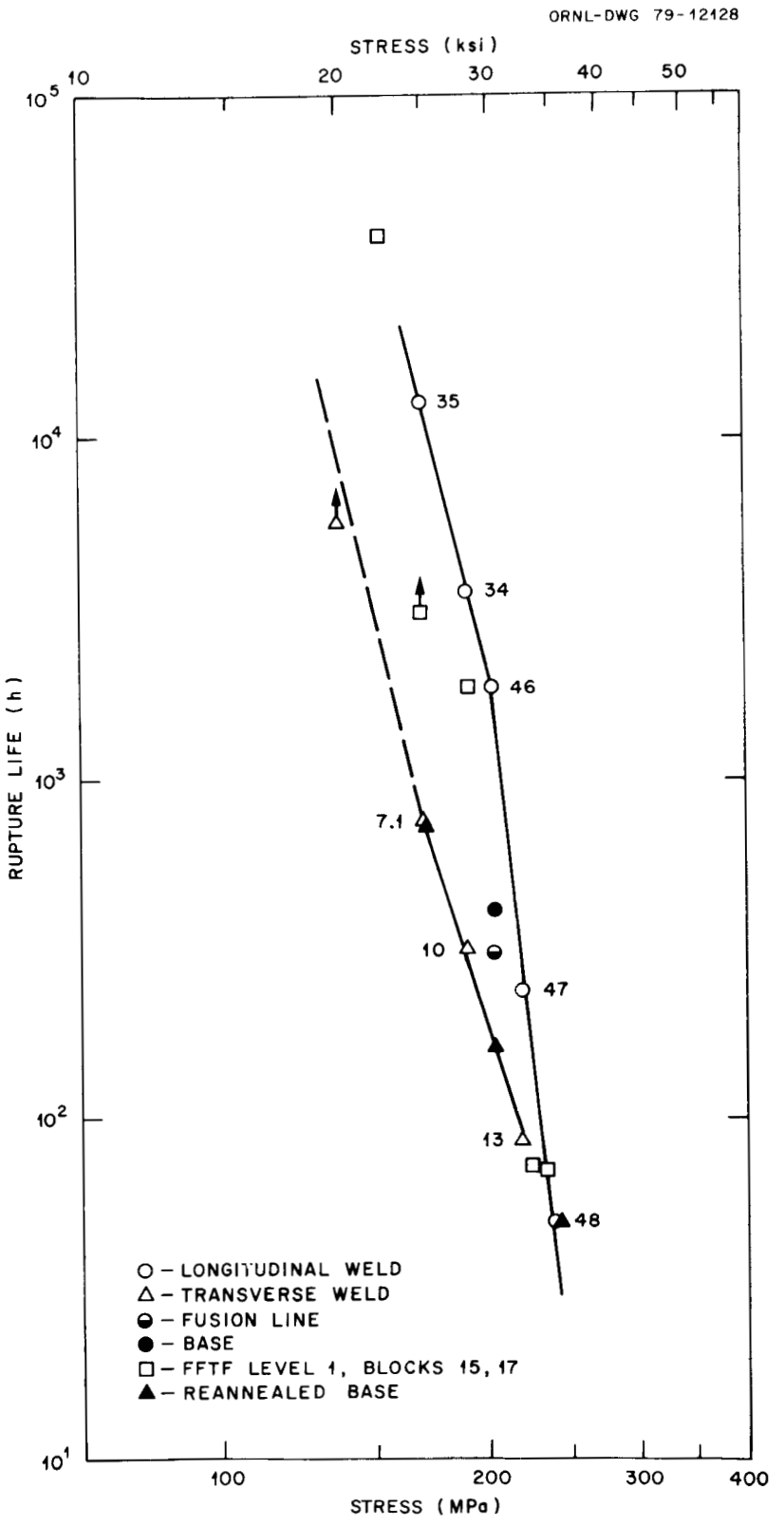

Fig. 10. Variation of Rupture Life with Stress and Location for Type 308 CRE Weld in 13-mm (1/2-in.) Plate of Type 304 Stainless Steel.

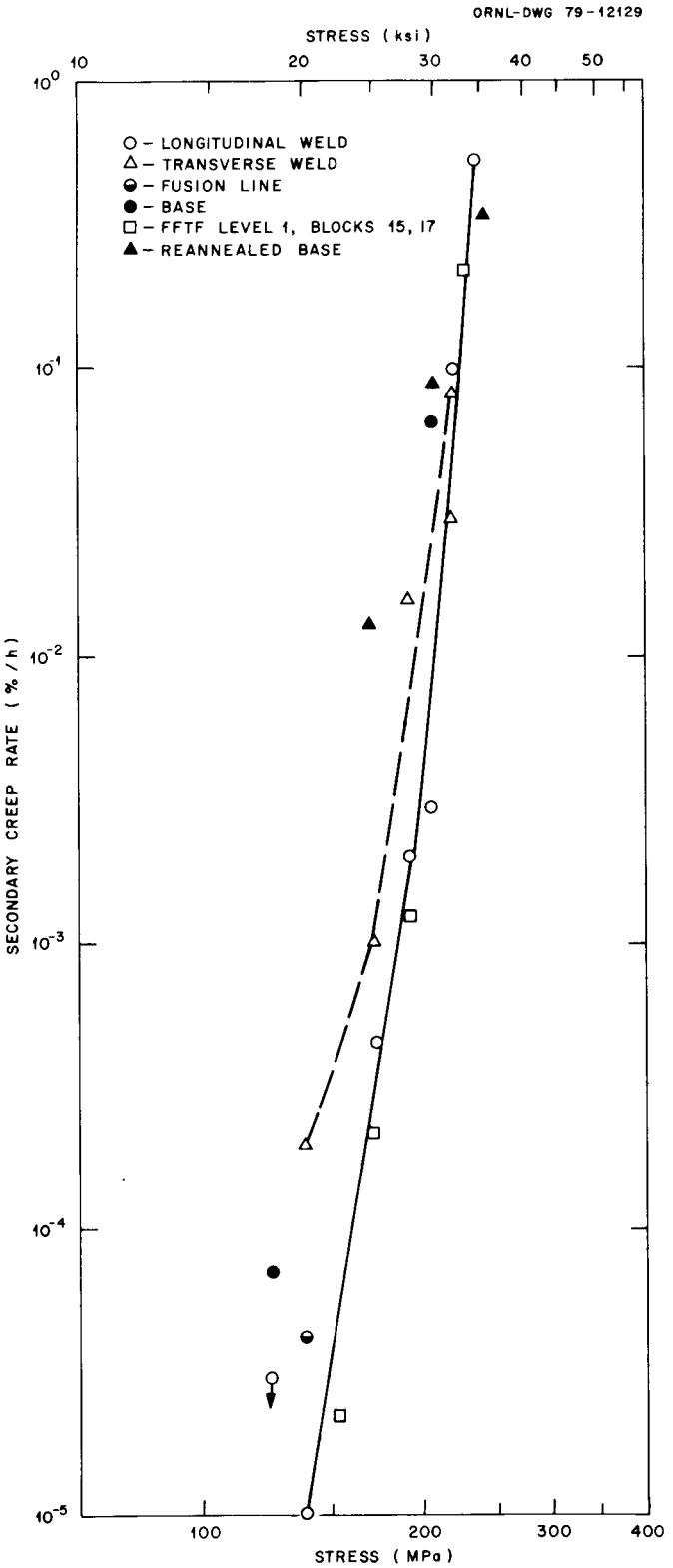

Fig. 11. Variation of Secondary Creep Rate with Stress and Location for Type 308 CRE Weld in 13-mm (1/2-in.) Plate of Type 304 Stainless Steel.

compared these data were equivalent to secondary creep rate data for level 1 FFTF material. Figure 12 also includes data for the reannealed 13-mm (1/2-in.) plate. This material was very weak.

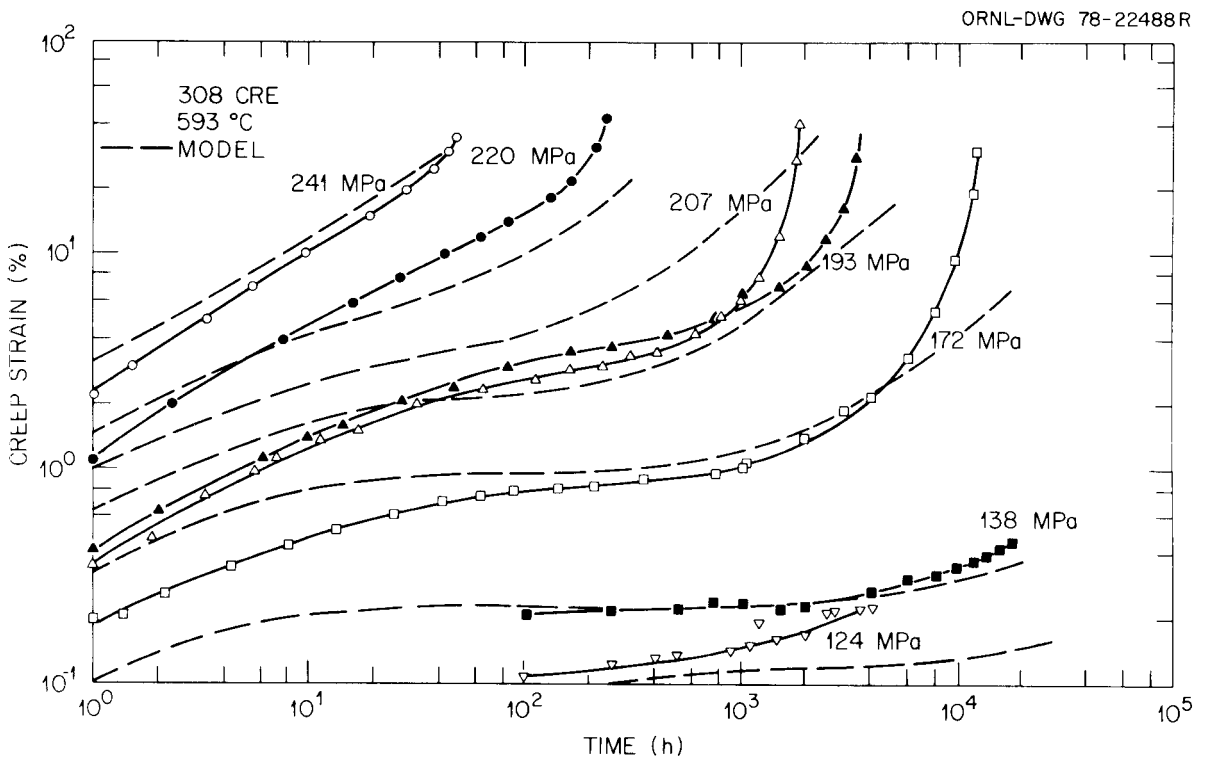

Fig. 12. Creep Curves for Type 308 CRE Weld Metal at 593°C (1100°F) in the Longitudinal Direction. Dashed lines are a suggested representation based on an analytical expression.

Representation of the Creep Curve

The seven creep tests on longitudinal weld specimens exhibited some inconsistency, which can best be seen in a plot of log strain versus log time. Data are presented in Fig. 12. The curves for specimens stressed at 207 and 193 MPa (30 and 28 ksi) fell close to one another and did not diverge until after 3.6 Ms (1000 h). At the lowest stresses the curves for specimens stressed at 124 and 138 MPa (18 and 20 ksi) tended to converge around 18 Ms (5000 h). With these exceptions the curves exhibited fairly well-defined trends. At short times and high stresses the slopes of the log of creep strain versus log of time curves were around 2/3. As

the stress decreased, the slope of the curves decreased. For example, at 172 MPa (25 ksi) the slope was close to 1/3. All curves for stresses below 241 MPa (35 ksi) turned downward after 36 ks (10 h), and the low-stress curves became very flat. Eventually, the curves turned sharply upward. The downward curvature suggested the need for a transient type expression for creep strain e versus time t in the primary stage. To "capture" the shallow slope of the log e versus log t curves in an analytical equation at short times, we resorted to a modification of the exponential form:

$$e_c = e_t[1-\exp(-rt)]^{\alpha} + \dot{e}_s t \quad , \tag{1}$$

where

e_c = creep strain;
e_t = transient strain asymptote;
r = transient strain rate parameter;
$\dot{e}_s$ = secondary creep rate, %/h;
α = parameter (which we selected to be 1/2).

We found that we could represent $\dot{e}_s$ as an exponential function of stress:

$$\dot{e}_s = \begin{matrix} 2.83 \times 10^{-12} \exp(0.108\sigma) & \text{(MPa)} \\ 2.83 \times 10^{-12} \exp(0.743\sigma) & \text{(ksi)} \end{matrix} \quad , \tag{2}$$

and e_t had a power dependence on stress:

$$e_t = \begin{matrix} 3.92 \times 10^{-15}\ \sigma^{6.43} & \text{(MPa)} \\ 9.66 \times 10^{-10}\ \sigma^{6.43} & \text{(ksi)} \end{matrix} \quad . \tag{3}$$

Finally, the product $e_t r$ was related to $\dot{e}_s$ by the equation:

$$e_t r = 1.07\ \dot{e}_s^{\,1/4} \quad . \tag{4}$$

Plots of these expressions are compared to data in Figs. 13, 14, and 15. Equations (2), (3), and (4) were introduced into Eq. (1), and creep curves

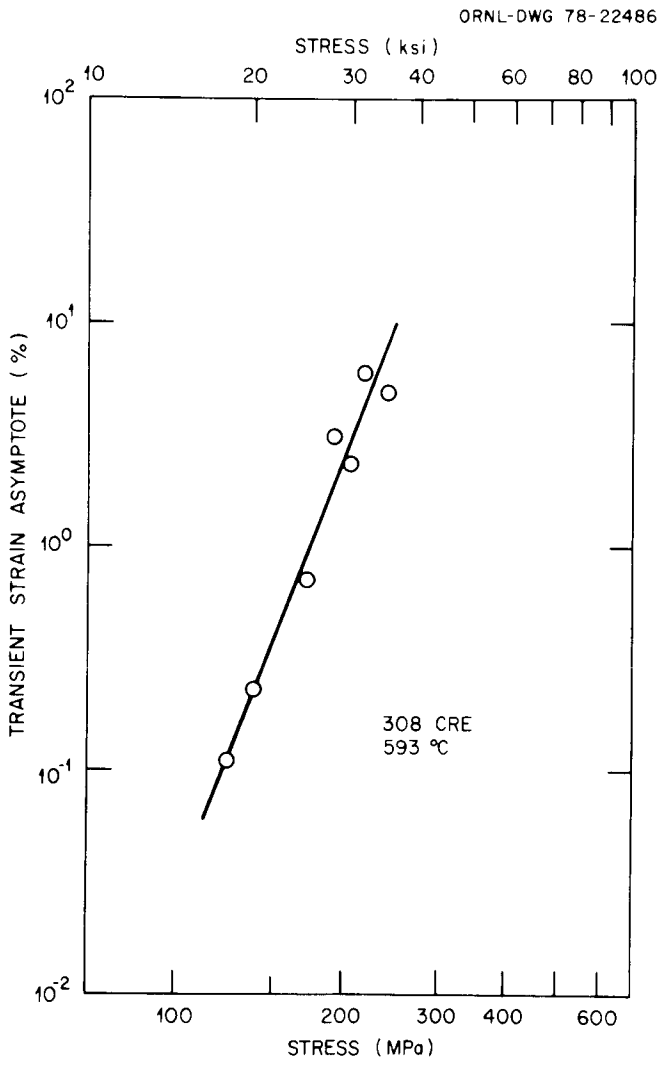

Fig. 13. Transient Strain Asymptote vs Stress for Type 308 CRE Weld Metal at 593°C (1100°F).

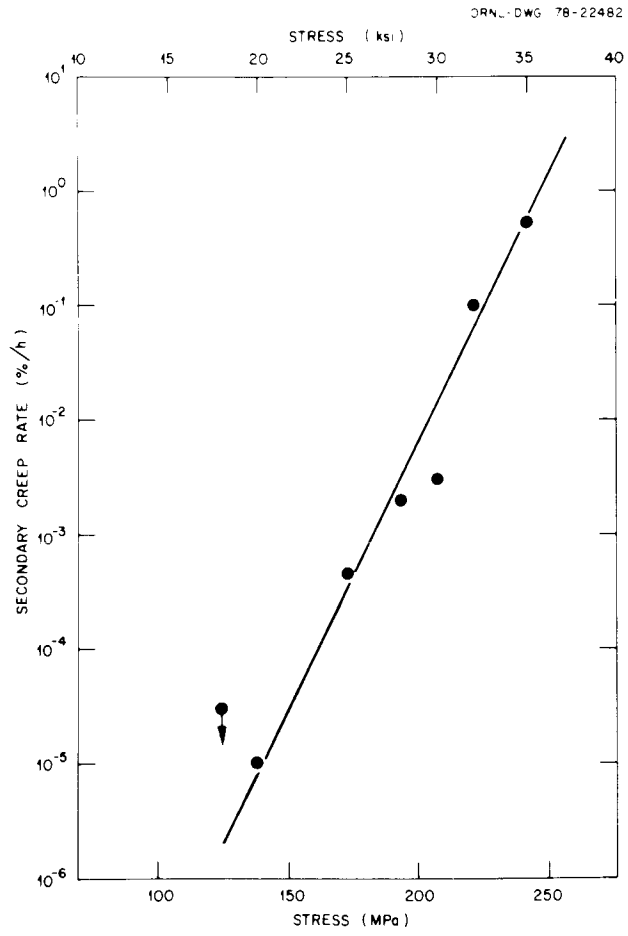

Fig. 14. Secondary Creep Rate vs Stress for Type 308 CRE Weld Metal at 593°C (1100°F).

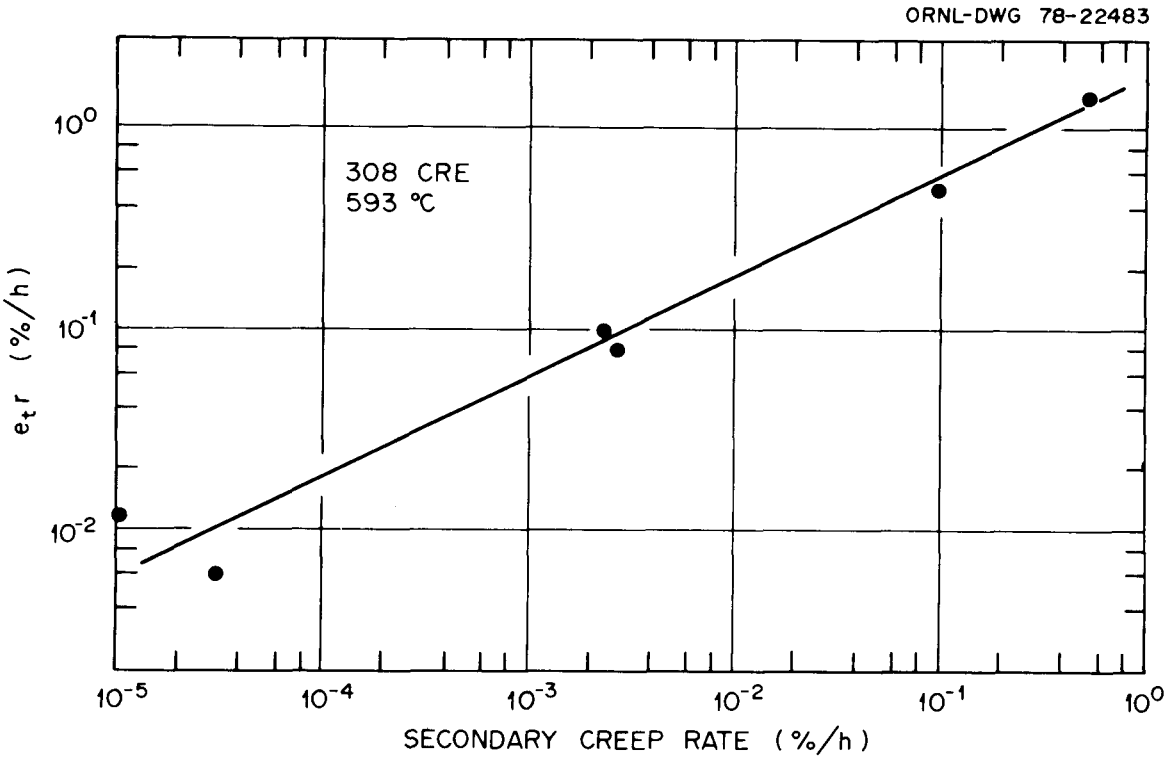

Fig. 15. Correlation Between $e_t r$ and Secondary Creep Rate for Type 308 CRE Weld Metal at 593°C (1100°F).

were calculated for several stresses. The curves are compared to data in Fig. 12. See curves labeled "model" for Eq. (1) representation. This comparison revealed that Eq. (1) overpredicted the short time strains. This could be fixed by increasing α from 1/2 to 3/4. However, we did not think that this step was needed in view of the inconsistency of the experimental data.

Log e versus log t curves for the transverse weld specimens, fusion-line specimens, and base metal specimens are provided in Fig. 16. Again the high-stress curves exhibited slopes near 2/3, while the low-stress curves exhibited slopes near 1/3. However, in the first 36 ks (10 h), the strains in the longitudinal weld specimens were about five times higher than strains in the transverse weld specimens. At 3.6 Ms (1000 h) strains were five times greater in the transverse weld specimens. This crossover resulted from the transverse and fusion-line specimens not noticeably turning downward at times beyond 36 ks (10 h). This difference is illustrated by the comparison of the curves for the specimens stressed

to 138 MPa (20 ksi) in Fig. 16. The downward curvature in the longitudinal weld specimen produced an order of magnitude difference in the strain at 36 Ms (10,000 h) that was between transverse and longitudinal specimens. Thus, both the "shape" and "position" of the log e versus log t curves varied with location of the specimen in the weldment. Therefore, the analytical representation for creep in the longitudinal specimens could not be directly applied to the fusion-line and transverse weld metal orientations without introducing major errors.

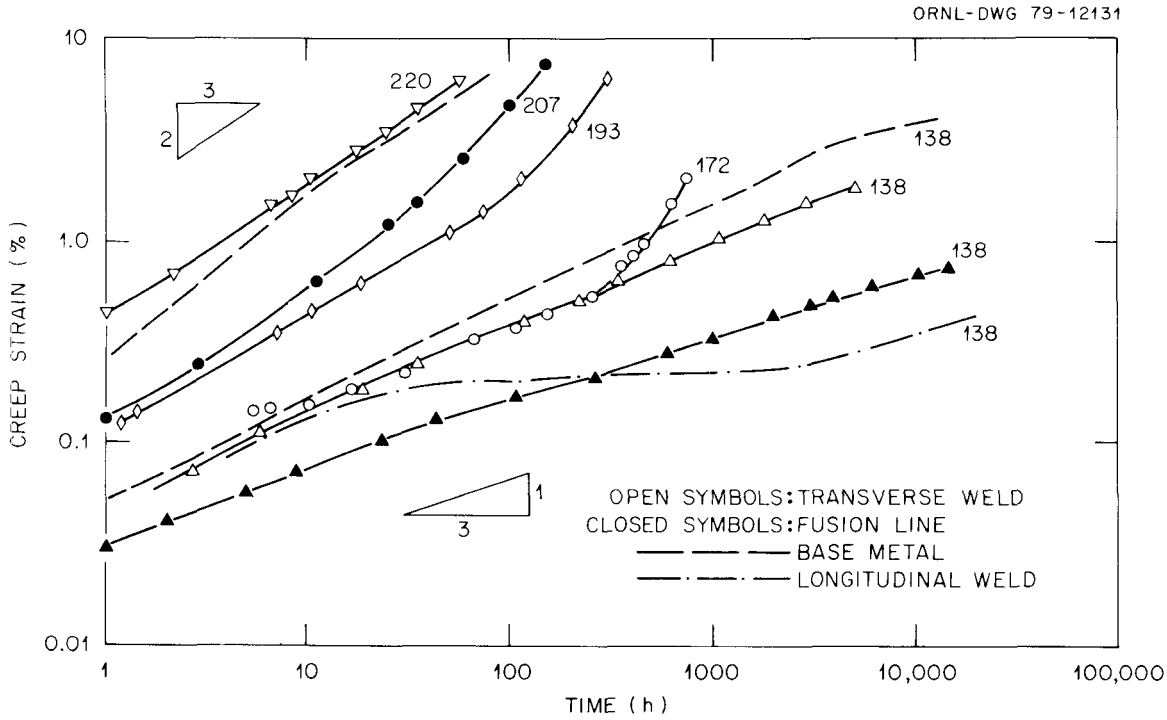

Fig. 16. Creep Curves for Transverse Welds and Fusion-Line Specimens at 593°C (1100°F).

DISCUSSION

As mentioned in the Introduction, the data reported here were gathered to characterize a material being tested in the Westinghouse Advanced Reactor Division (WARD) Validation Program. As part of this effort, M. J. Manjoine is creep testing type 304 stainless steel plate specimens with longitudinal and transverse welds. Both deformation and rupture behavior is of interest. It is not obvious that data for the small specimens that we examined can be directly applied to the analysis

of weldment behavior. Nevertheless, it does seem likely that if we can understand the behavior of specimens machined from the composite, we will have a better chance of understanding how the composite weldment will behave.

Let us first consider the relative behavior of the longitudinal and transverse weld specimen. The plastic flow stress of transverse weld specimens is higher than the flow stress of longitudinal specimens (Figs. 8 and 9). Furthermore, the transverse weld specimens have greater creep strength during the early stages of creep (Figs. 12 versus 16). The longitudinal weld orientation has a greater uniform strain under tensile straining (Fig. 8) and a greater "true ultimate strength" (see Table 2). Under creep-rupture the longitudinal weld specimens exhibit lower secondary creep rates, much greater ductilities, and better rupture strengths than the transverse orientation specimens (Figs. 11 and 12). Why does this happen? We can explain the shorter rupture life and lower ductility of the transverse weld material on the basis that the transverse weld specimens rupture in the "weaker" base metal. However, most of the material in the transverse weld specimens is weld metal, and we might expect that the deformation behavior of transverse weld specimens would be controlled by the weld metal deformation properties. King et al.[4] working on FFTF welds report the same dependence of creep behavior on specimen orientation as seen in the WARD weldments. Yet they also show that the elastic properties of weldments are isotropic in the plane of the plate and vary as the orientation changes from the plane of the plate to the axis perpendicular to the plate.[9] This observation makes sense because the columnar grains have their [100] axis perpendicular (90°) to the plate surface but are randomly oriented about the axis normal to the plate surface. In the WARD transverse weld specimens the columnar grains start out inclined at an angle 68° to the plate surface but "rotate" to 90° in a short distance. Hence, it seems likely that the behavioral difference in the transverse and longitudinal oriented specimens is not entirely affected by crystallographic or grain shape but is rather partly influenced by the directional strains introduced during welding. The strains introduced in welding must be very large. King et al.[4] report a dislocation line density of $10^{10}/cm^2$ for material near the surface of the FFTF welds. This

density is an order of magnitude greater than the density observed in annealed material and corresponds to the density produced by monotonic strains in the range 5 to 10%. Although we can expect that such strains would harden isotropically, there could be some kinematic or directionality effects. Possibly, this directionality is what produces the orientation dependence of weldment behavior. This explanation could be checked by stress-relieving the welds and reevaluating the properties in the transverse and longitudinal directions.

The difference in creep response is somewhat puzzling. The larger plastic loading strains, which should occur in the longitudinal weld specimens at the start of the creep test (Fig. 9), should also harden the material to a level comparable to the transverse weld specimens. Therefore, we are at a loss to explain why the initial creep rate for longitudinal specimens is a factor of 5 greater than the rate for transverse weld specimens. Since the tests at 138 MPa (20 ksi) plotted in Fig. 16 do not show this factor of 5 difference at short times, we might resort to the explanation that experimentally "creep" and "plastic" strains are difficult to separate at the start of a creep test. Thus, the difference in the initial creep rates of longitudinal and transverse specimens may not be real. The much lower secondary creep rates in the longitudinal weld specimens (Fig. 11) could be explained by the increasingly greater effects of the base metal on the transverse weld specimens as the creep test progresses. For example, the ratio of the initial creep rate to "secondary" creep rate in longitudinal welds is of the order of at least 1000 at lower stresses. A similar ratio could apply to transverse weld material. The base metal in the transverse weld specimen could exhibit less hardening. Hence, as the creep test continues the base metal contribution to the creep of the transverse specimen becomes greater. Grain boundary sliding and wedge cracking in the base metal could also contribute to what appears to be a higher secondary creep rate in transverse weld metal specimens.

It is fairly clear that a key to understanding the behavior of the transverse weld specimens would be to study the influence of prior strain on subsequent creep and rupture behavior. Efforts should be made to introduce defect structures typical of the base metal near the weld. We

should then study the creep and ductility relative to all-weld metal specimens.

In this discussion we have not examined the influence of δ-ferrite, sigma formation, or the influence of carbide precipitation phenomena on creep and rupture. These are all important metallurgical considerations that have been discussed by King and co-workers[4,6–8] for the FFTF welds.

CONCLUSIONS

1. The type 308 CRE stainless steel welds produced for WARD are weaker than the level 1 FFTF material under tensile testing at 593°C (1100°F).

2. Longitudinal weld specimens are weaker than transverse weld specimens for tensile strains in the range 1 to 15%. Longitudinal weld specimens exhibit higher uniform strains.

3. The longitudinal weld specimens exhibit rupture lives equivalent to the level 1 FFTF material. Creep ductilities are high.

4. The transverse weld specimens exhibit rupture lives that are much less than the longitudinal weld specimens. The strength is comparable to the weak base metal heat (9T2796). Creep rupture occurs in the base metal, and the total elongations are low.

5. The creep behavior of the longitudinal weld metal specimens can be modeled by a modified exponential creep equation.

6. Efforts should be made to study the effect of the strains produced during welding on the creep-rupture behavior of base metal near the weld.

ACKNOWLEDGMENTS

The authors are indebted to the reviewers J. W. McEnerney and K. C. Liu for helpful comments. The manuscript was edited by B. G. Ashdown and prepared by A. F. Rice.

REFERENCES

1. R. G. Gilliand, *The Behavior of Welded Joints in Stainless and Alloy Steels at Elevated Temperatures,* ORNL-4781 (August 1972).

2. N. C. Binkley, G. M. Goodwin, and D. G. Harman, "Effects of Electrode Coating on Elevated-Temperature Properties of Austenitic Stainless Steel Weld Metal," *Weld. J.* 52: 306-s—311-s (1973).

3. T. J. Delph, "Structural Design Methods for Weldments," *High-Temperature Structural Design Program Semiannu. Prog. Rep. June 30, 1978,* ORNL-5433, pp. 227—48.

4. R. T. King, J. O. Stiegler, and G. M. Goodwin, "Relation Between Mechanical Properties and Microstructure in CRE Type 304 Weldments," *Weld. J.* 53: 307-s—313-s (1974).

5. M. J. Manjoine, *Basic Creep-Rupture Testing at 1100°F (593°C) of Type 304 Stainless Steel for Uniaxially Loaded Specimens with Stress and Strain Gradients,* WARD-HT-3045-26 (June 1977).

6. N. C. Binkley, R. G. Berggren, and G. M. Goodwin, "Effects of Slight Compositional Variation on Type E308 Electrode Deposits," *Weld. J.* 53: 91-s—95-s (1974).

7. R. T. King, J. O. Stiegler, and G. M. Goodwin, "Creep Properties of a Type 308 Stainless Steel Pressure Vessel Weld with Controlled Residual Elements," p. 181.1 in *Creep and Fatigue in Elevated Temperature Environments,* Institution of Mechanical Engineers, London, 1975.

8. R. T. King, J. O. Stiegler, and G. M. Goodwin, *Properties of Thick Type 308 Stainless Steel Welds with Controlled Residual Elements,* ORNL/TM-4206 (June 1974).

9. B. R. Dewey, L. Adler, K. V. Cook, and R. T. King, "Measurements of Anisotropic Elastic Constants of Type 308 Stainless Steel Electroslag Welds," to be published in *Experimental Mechanics.*

10. C. R. Brinkman and G. E. Korth, *Heat-to-Heat Variations in the Fatigue and Creep-Fatigue Behavior of AISI Type 304 Stainless Steel and the Fatigue Behavior of Type 308 Stainless Steel Weld Materials,* ANCR-1097 (May 1973).

11. V. Provenzano, J. R. Hawthorne, and J. A. Sprague, "Fractographic Analysis of Elevated Temperature Fatigue Crack Propagation in AISI Type 308 Weld Deposits," pp. 63—75 in *Properties of Steel Weldments for Elevated Temperature Pressure Containment Applications,* MPC-9, ed. by G. V. Smith, American Society of Mechanical Engineers, N.Y., 1978.

12. M. W. Williams, *Metallographic and Fractographic Observations of Posttest Creep-Fatigue Specimens of Weld-Deposited Type 308 CRE Stainless Steel,* ANL-78-74 (August 1978).

13. M. J. Manjoine, "Determination of Grain Distributions in a Creep Test of a Weldment at 1100°F," paper presented at Society of Experimental Stress Analysis Spring Meeting, Silver Springs, Md, May 9–14, 1976.

14. V. K. Sikka, R. W. Swindeman, M. K. Booker, B.L.P. Booker, and R. L. Stephenson, *Tensile Properties of Type 304 Stainless Steel,* ORNL-5325 (February 1978).

15. R. W. Swindeman, W. J. McAfee, V. K. Sikka, H. E. McCoy, Jr., and R. D. Waddell, Jr., *Product Form Characterization of Type 304 Stainless Steel (Heat 9T2796),* ORNL-5222 (February 1977).

ORNL/TM-6995
Distribution
Category UC-79b, -h, -k

INTERNAL DISTRIBUTION

1–2. Central Research Library
3. Document Reference Section
4–5. Laboratory Records Dept.
6. Laboratory Records, ORNL R.C.
7. ORNL Patent Section
8. J. J. Blass
9. E. E. Bloom
10. E. Bolling
11. M. K. Booker
12. C. R. Brinkman
13. J. A. Clinard
14–15. J. M. Corum
16. J. R. DiStefano
17. D. P. Edmonds
18. G. M. Goodwin
19. R. C. Gwaltney
20–24. M. R. Hill
25. R. L. Huddleston
26. R. T. King
27. R. L. Klueh
28. D. J. McAfee
29. J. W. McEnerney
30. H. E. McCoy
31. C. E. Pugh
32. W. K. Sartory
33. G. M. Slaughter
34. V. K. Sikka
35. J. O. Stiegler
36–45. R. W. Swindeman
46. G. T. Yahr
47. R. W. Balluffi (Consultant)
48. A. L. Bement, Jr. (Consultant)
49. J. F. Harvey (Consultant)
50. W. R. Hibbard, Jr. (Consultant)
51. E. H. Kottcamp, Jr. (Consultant)
52. M. J. Mayfield (Consultant)
53. E. T. Onat (Consultant)
54. J. T. Stringer

Subcontractors

55. H. Armen, Jr., Grumman Aerospace Corp., Bethpage, NY 11714
56. J. M. Chern, Foster-Wheeler Energy Corp., 110 S. Orange Avenue, Livingston, NJ 07039
57. C. E. Jaske, Battelle-Columbus Laboratories, 505 King Avenue, Columbus, OH 43201
58. W. J. O'Donnell, O'Donnell and Associates, 5100 Centre Avenue, Pittsburgh, PA 15236
59. S. Y. Zamrik, Pennsylvania State University, University Park, PA 16802

EXTERNAL DISTRIBUTION

60–61. DOE DIVISION OF REACTOR RESEARCH AND TECHNOLOGY, Washington, DC 20545

Director

62. DOE OAK RIDGE OPERATIONS OFFICE, P.O. Box E, Oak Ridge, TN 37830

Assistant Manager, Energy Research and Development

63–272. DOE TECHNICAL INFORMATION CENTER, Office of Information Services, P.O. Box 62, Oak Ridge, TN 37830

For distribution as shown in TID-4500 Distribution Category, UC-79b (Fuels and Materials Engineering Development); UC-79h (Structural Materials Design Engineering); UC-79k (Components).

☆ U. S. GOVERNMENT PRINTING OFFICE: 1979-640-245-276